IUG Journal of Natural Studies
Peer-reviewed Journal of Islamic University-Gaza

ISSN 2409-4587

IUGNES
Vol. 25, No 2, 2017, pp 10-20

Accepted on (14-03-2017)

Electrical Resistivity Tomography for Coastal Sea Water Intrusion Characterization along Rafah Area, South of Gaza Strip, Palestine

Zeyad H. Abu Heen[1,*]
Shehda A. Muhsen[2]

[1]Department of Environment & Earth sciences, Faculty of Science, Islamic University of Gaza, Gaza Strip, Palestine

[2]Ministry of Palestinian Education & Higher Education, Gaza Strip, Palestine

*** Corresponding author**
e-mail address: zabuheen@iugaza.edu

Abstract

Resistivity methods mainly electrical resistivity tomography 2D and resistivity sounding 1D represent the main geophysical tools to delineate seawater intrusion into freshwater aquifers. Thirty 2D imaging sections were applied with Wenner-Schlumberger array (NW-SE direction), distributed on six profiles (perpendicular to the coast) in southern part of the coastal aquifer in Gaza Strip (Rafah Governorates), supported by 4 Vertical electrical soundings points with Schlumberger array, to map shallow-depth seawater intrusion into freshwater aquifer and study the subsurface geologic formation. Analysis and interpretation of the electrical resistivity tomography 2D and 1D sounding results reveal that seawater intrusion zone appears at the western part of the study area and extends along Rafah coast with a difference distance and depths. The depths are ranging between (few meters to 20 m) in the western sections, while they are betwee 40 to more than 65 m in the eastern section. The resistivity data results were correlates well with the 3 boreholes data and 3 chemical analyses water samples.

Keywords:
Electrical resistivity tomography 2D,
VES,
1D,
Seawater intrusion,
Rafah,
Gaza Strip,
Palestine.

1. Introduction:

In coastal areas sea water intrusion into fresh groundwater aquifers causes many acute environmental problems. The extent of saline water intrusion may vary between a few meters to kilometers, and it is mainly controlled by the geological formations (Himi et al., 2010), aquifer type, thickness and hydraulic conductivity of the aquifer, climate conditions, ground water level with respect to mean sea elevation (Chachadi and Ferreira, 2005).

Groundwater coastal aquifer is considered the main natural source of fresh water supply for all activities (domestic, irrigation and industrial supply).

Groundwater is the main source of water in Gaza Strip and considered the only natural source of fresh water supply for all activities. Water analysis results revealed that more than 90% of the water wells unsuitable for domestic uses according to WHO Standards. The water sector suffers many problems in terms of quantity and quality. (Abu Heen et al., 2008; Abu El-Naeem et al., 2009). Electrical resistivity methods have been widely used to study groundwater contamination. The decrease in resistivity caused by salinity of groundwater helps to identify the contaminant zones.

Surface resistivity methods have been used for groundwater research for many years. Earth resistivities are related to important geologic parameters of the subsurface including types of rocks and soils, porosity and degree of saturation. It was shown that the electrical resistivity of rocks and minerals, except for massive sulfides and graphite, vary in a wide range between 1 to 107 ohm-m, whereas coastal aquifers that are brine to saline water are identified by relatively low resistivity values. Thus, saltwater can be easily distinguished from almost any combination of lithological types.

A number of outstanding papers and reports have been published on the application of geophysical techniques (electrical resistivity 1D and 2D) to delineation seawater intrusion with aquifer coastal such as Keller and Frischknecht (1966); Zohdy et al. (1974); Gemail et al. (2004); Choudhury et al. (2004); Sherif et al. (2006); Al-Bassam et al. (2008); De Franco et al. (2009); Capizzi et al. (2010); Batayneh et al. (2010); Chitea et al. (2011); Olympia et al. (2012); Lagudu et al. (2013); Thabit et al. (2014); Basheer et al. (2014); Kalisperi et al. (2015); Mogren (2015); Muhsen (2016) and Abu Heen and Muhsen (2016).

The fundamentals of resistivity method is based on passing electrical current into ground surface by two current electrodes, and the potential difference is measured between a second couple of electrodes. These measurements are inverted into a distribution of electrical resistivity in the subsurface. The resistivity boundaries are interpreted in terms of lithological boundaries, the foundation of this is Ohm's law.

A more accurate model of the subsurface is a two-dimensional (2-D) model where the resistivity changes in the vertical direction, as well as in the horizontal direction along the survey line (Loke, 2004; Dahlin and Zhou, 2004; Loke, 2011).

2. Geological and Hydrogeological Setting of the Study Area:

The study area is located along the Gaza coastal plain, in the southern part of Gaza with longitudes 34° 2" and 34° 25" east, and latitudes 31° 16" and 31° 45" north (Figure 1).

The total area of Gaza Strip is about 365 km^2 and its length is approximately 45 km along the coastline and its width ranges from 6 to 13 km and some of about 2 million inhabitants (PCBS, 2016).

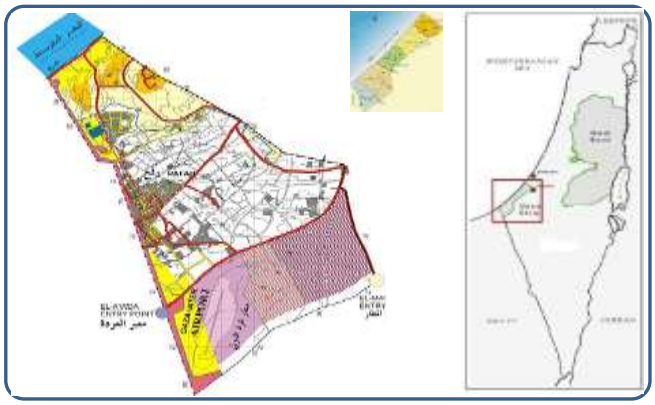

Figure 1 *Location map of the study area (Rafah Governorates)*

Topography of the study area (Rafah Govornorates) is characterized by Land surface elevation ranges from zero to about 100 m above mean sea level. Geologically, the study area is a shore plain gradually sloping to the west. It is underlain by a sequence of geological formations ranging from upper Cretaceous to Holocene (Figure 2). The main formations known were composed in the last two system periods, Tertiary formation called "Saqiya formation" of about 1200-meter thickness, composed of shallow marine impervious sediments of Shale, Clay, and Marl wedged out rapidly to the east ,and the Quaternary deposits of about 160 meters thickness and cover Saqiya formation. The coastal aquifer composed of loose sand dunes (Holocene age) and Kurkar group (Pleistocene). The Kurkar group composed of marine and aeolian calcareous sandstone (locally known as "Kurkar"); reddish silty sandstone ("hamra"; silts, interlayers of clay deposited (Metacalf & Eddy, 2009).

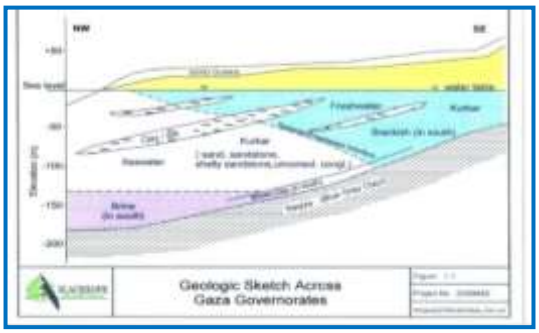

Figure 2 *Hydrogeological cross-section of the coastal aquifer (Metacalf & Eddy, 2009)*

The majority of fresh water supplies in Gaza Strip come from groundwater resources (PWA, 2015a, 2015b).

Future population growth and its associated water demands are expected to place severe pressure on these limited groundwater reserves. Factors that contribute to water contamination in the Gaza Strip include seawater intrusion, wastewater, overuse of agricultural pesticides and fertilizers, and solid waste that might produce toxic substance, e.g. nitrate (Yassin et al., 2006; Agha, et al., 2005; Al-Absi, 2008; Abu El-Naeem et al., 2009; Shomar, 2010).

In study area (Rafah) there is a clear deterioration in groundwater quality. The total groundwater production reached in 2014 to about 9.7 million cubic meters, and thus the average water consumption of water production total is 120/liter/capita/day, taking into account the efficiency of network distribution not more than 63%, so the average per capita is 75/liter/capita/day, that is not recommended internationally (PWA, 2015b).

Further contaminates groundwater (increase in nitrate level) comes from underdeveloped wastewater storage and treatment facilities and unchecked sewage flow in the Gaza Strip and nitrates from uncontrolled sewage, and fertilizers from irrigation of farmlands. Amount of untreated or partially treated wastewater that is dumped 90,000 CM per day or 33 MCM per year (UNCT, 2012).

Seawater intrusion and intensive exploitation of groundwater have resulted in increased salinity in most areas in Gaza Strip especially along the Gaza border in the middle and south areas with concentrations exceeding 1000mg/l. The best water quality(50–250mg/l) is found in the sand dune areas in the north (PWA, 2013a, 2013b, 2014, 2015a, 2015b). Chloride concentration of the groundwater that supplied for Gaza people from the municipal wells in 2014 was ranging from 250 to more than 5000 mg/l. 9.5 % of that has chloride concentration of less than 250 mg/l (WHO allowable limit), while the remaining (90.5%) exceeds the WHO chloride level as shown in Figure 3. The figure shows that most of the study area (Rafah governorate is characterized by poor quality of chloride concentration, especially in the western region that extended from north-west of the governorate and even the south west to more than 5 km within the coastal strip.

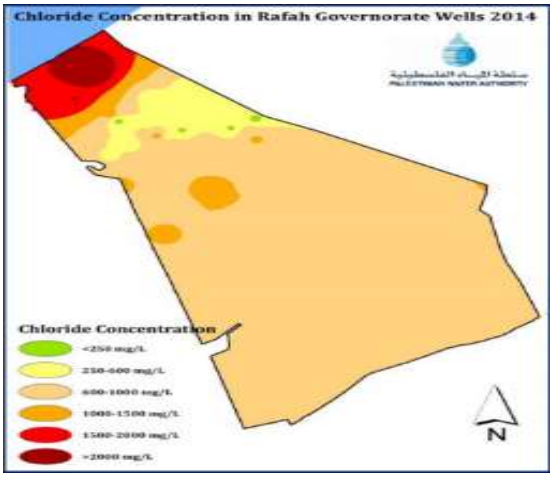

Figure 3 *Chloride concentration map in Rafah (PWA, 2015b)*

3. Materials and Methods:

To delineate the boundaries between seawater intrusion and subsurface fresh groundwater aquifer in the study area, some of (30) 2D resistivity imaging sections were carried out using Wenner-Schlumberger array with a NW-SE direction, distributed on six profiles in the study area as shown in Figure 4. Syscal R1 Plus Switch-24 resistivity instrument of Iris, France, with 24 electrodes is used. The distance between the electrodes is 5m, so the total cable length is 120m, while the total measured spread is 115m long. The 2D profiles supported by (4) vertical electrical sounding (VES) measuring points with Schlumberger array and current electrodes (AB/2) are 2, 3, 4, 5, 6, 8, 10, 13, 16, 20, 25, 30, 40, 50, 60, 80, 100 and 130m, and (MN/2) varying from 0.25 to 16 m. in order to determine the number of the underlying layers, depths, thicknesses and their conductivity.

The interpretation of 2D resistivity imaging is completed by using (Res2dinv) program (Geotomo software, 2010). While the interpretation of vertical electrical sounding (VES) points is carried out automatically by using the (IPI2Win) Software (Bobachev, 2010). Litholgy data obtained from two boreholes, where these lithological data provide a very important constrains on the results of the sounding data and profiling interpretation.

To study the hydrochemical parameters of the groundwater of the study area, three chemical water samples analyses results were collected from three agriculture wells to confirm the VES results (Table 1).

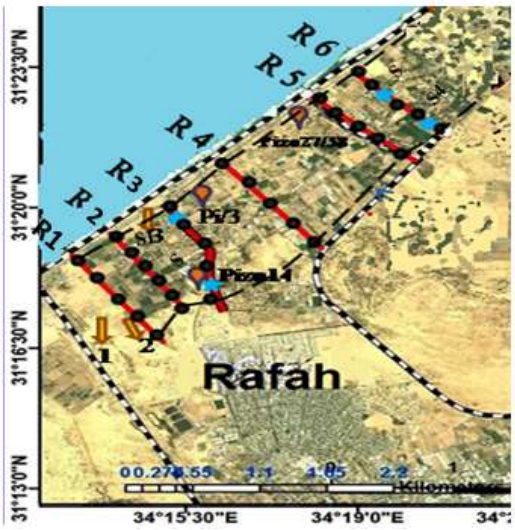

▬	Profile Line
●	2D Profiling
★	1D Sounding
	Borehole log
	Water well

Figure 4 *Location map of 2D resistivity tomography profiles*

Table1 *Results of hydrogeochemical analysis of groundwater in the study area*

Well No.	Well name N	Well name E	EC µS /cm	TDS mg/l	CL mg/l	Na mg/l
1	31⁰ 18' 58.72"	34⁰ 13' 28.82"	5200	3302	1469.5	544.5
2	31⁰ 19' 05.93"	34⁰ 13' 36.70"	7300	4635	2109.3	732.9
3	31⁰ 18' 34.46"	34⁰ 13' 33.03"	7900	5016	2149.3	906.9

4. Results and Discussion:

4.1. 2D Resistivity Tomography Interpretation

- **Profile (R1):**

Profile R1 was carried out south Rafah (Figure 1) and consists of four sections (R1-1, to R1-4) as shown in Figure 5.

The inversion results of this profile data indicate that resistivity values gradually change horizontally in profile R1 from west (Sea coastal) to east, and gradually change vertically with increasing depths.

Inspection Figure 5 reveals that the top layer reflect high resistivity values (>100 Ωm), that may reflects the presence of coarse-grained sediment sand on the surface. The second layer is characterized by a relatively low resistivity varying between (8-16 Ωm) in the subsurface, may reflects the increase clay content in the fresh aquifer.

The image illustrate that the inversion result indicates lower electrical resistivity values, with a resistivity of less 2 Ωm, were observed at a depth of 3 m at 80 m mark to 6 m depth at the western side of

R1-1 near the coast line and extend along the section R1-1 and R1-2. The reduced values may be due to saturated strata of subsurface seawater flow zone.

Section R1-3 shows the same feature, where brackish water (less than 3 Ωm) saturated the kurkar aquifer at depth of about 6.7m at mark 360 m, but at more depth eastward to about 10m at 420 m mark.

Seawater intrusion can be observed in section R1-4, where resistivity values decreases to less than 2 Ωm at depth of about 16m in all the sections. Further, the lower resistivity was confirmed by chemical analyses for the nearby agriculture water well no. 1 (Table 1) where EC equal to about 5200 µS /cm.

- **Profile (R2):**

Profile R2 extended to about 800 m from west to east and located about 600 m to the north of profile R1, nearly parallel to it, and consist of five sections (from R2-1to R2- 5), as shown in Figure 1.

The inversion results of this profile Figure 6 indicate that top soil layer are characterized by high resistivity values at different depths and, in general, the resistivity values increased from west to east that reflect the change in surface soil type.

A thick conductive layer (of about 12 m thick) is well observed along section R2-1 with resistivity values less than 2 Ωm that represent the seawater intrusion in sandstone layer. Towards east direction (R2-2) this conductive layer becomes more resistivity (between 7 and 55 Ωm) that reflect fresh to brackish water intruded into the aquifer.

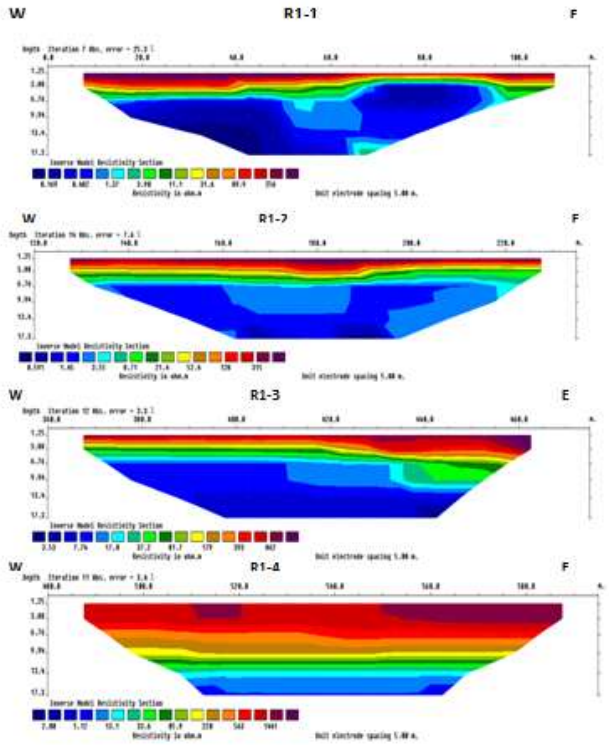

Figure 5 *2D Electrical resistivity images along profile R1*

Seawater intrusion observed at the eastern end of R2-2 at depth of about 13m extends from 330 m mark to 430 m mark (R2-3). High resistivity anomaly of more than 400 Ωm up to 770 Ωm is observed at mark 460 to 500 m mark (R2-3), that extends up to mark 620 m mark (R2-4) and to the end of section R2-5 for a depth of about 3m to about 12m.

Avery brackish layer with resistivity values less than 5 Ωm is dominant under all R2-4 section at depth of about 13 m which mean that the salinity increased also from west to east direction at lower depth.

The resistivity profile was correlated with chemical analyses for the nearby agriculture water well no. 2.

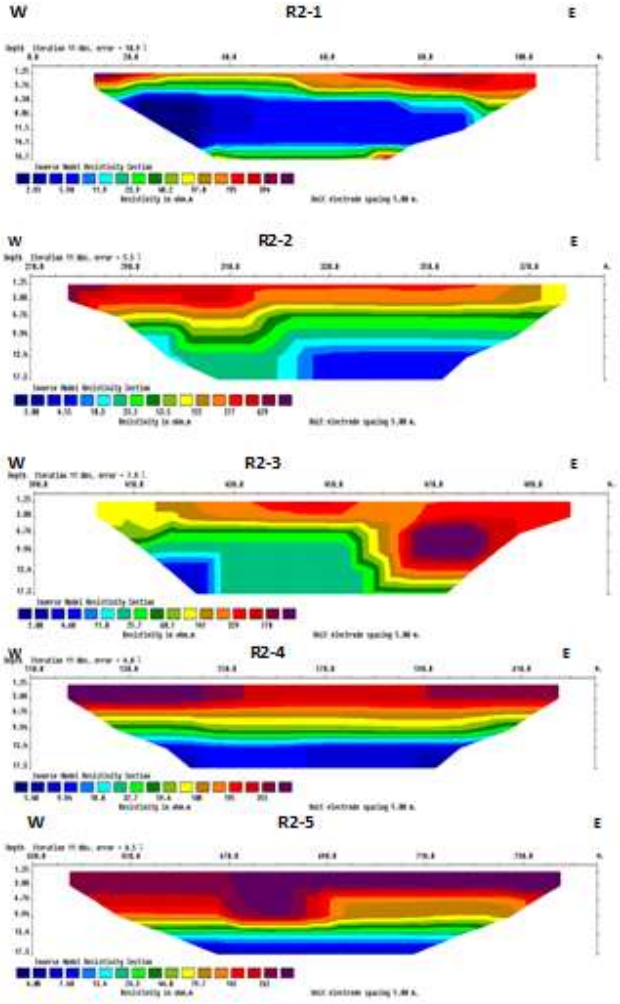

Figure 6 *2D Electrical resistivity images along profile R2*

- **Profile (R3):**

Profile R3 consists of five section (from R3-1 to R3- 5) extended to about 1000 m in east – west direction and located about 600m to the north of profile R2, and parallel to it Figure1. The interpreted 2D geoelectrical model is illustrated in Figure 7. It is shown that resistivity values gradually change horizontally from the west to the east, where the range (> 220 Ωm) in the west and reduced to (100 Ωm) to the east, due to the topsoil difference where an incoherent moderate grained sediment sand is characterized by high resistivity east to the coast line covered by agricultural land which characterized by low resistivity due to increase clay and silt content.

Generally, apparent resistivity values are decreasing gradually with increasing the depth.

The second layer is characterized by a relatively high resistivity varying between 3 Ωm to 50 Ωm at depths

between 5 to more than 16.7m which may reflect a Kurkar aquifer saturated with brackish water. However, section (R3-1) illustrates the seawater intrusion with resistivity values less than 2 Ωm reveals at the section bottom at depth of about 11 m (near the coast) to depth of about 16m at 60m mark eastwards. Underlying this layer is a lower resistivity zone (1-4.7 Ωm) which represents sand layer saturated with saline water as propose by borehole Pi/3 description Figure 10.

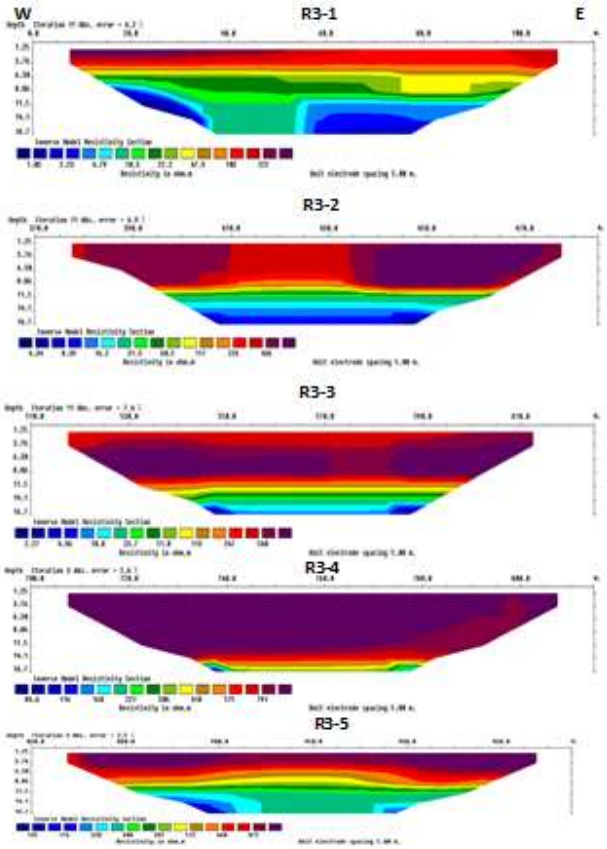

Figure 7 *2D Electrical resistivity images along profile R3*

The interpreted geoelectrical model of section R3-1 was confirmed with chemical analyses for the nearby agriculture water well no. 3 (Table 1) and with interpretation of 1D models of sounding no VES S1and VES S2 (Figures 8 and 9) and borehole Piezo 14/82 and Pi/3 (Figure 11).

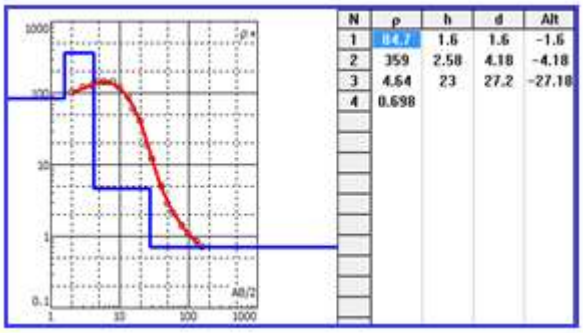

Figure 8 *1D geoelectrical model of VES S1*

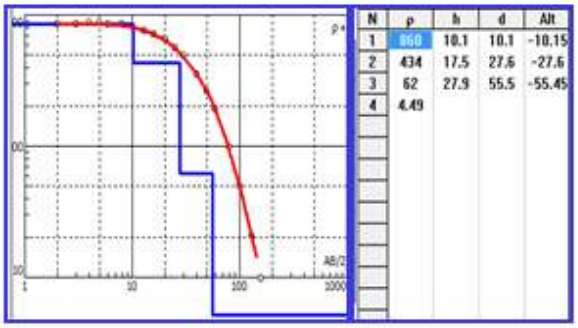

Figure 9 *1-D geoelectrical model of VES S2*

- **Profile (R4):**

Profile R4 was carried out nearly north of profile R3 at distance of about 600m and consists of six section (R4-1, to R4- 6) and extends to about 1100 (Figure 1).

The inversion results of profile R4 (Figure 11) show apparent resistivity value ranges from less than 0.8 Ωm to more than 1106 Ωm. The top layer characterized by high resistivity values along all the profile, to the presence of grained sediment sand on the surface.

Top soil formation overlay a resistivity formation with resistivity values range between (8-16 Ω m) in the subsurface that may due to clay layer and/or saturated with brackish water.

The inversion result of R4 profile indicates that sea water intrusion is observed at depth up to 17 m at R4-1 and at shallower depth (about 15m) under R4-2 and R4-3, but not observed after 600m east of the coast line (R4-4, R4-5 and R4-6). The dominant aquifer layer in R4-4, R4-5 and R4-6 characterized by medium to high resistivity values that reflect fresh water (Abu Heen and Muhsen, 2016).

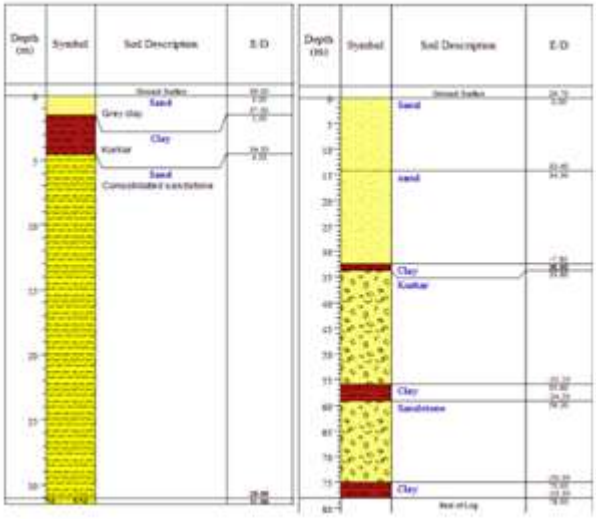

Figure 10 *Lithology of borehole logs of Piezo 14/82 and Pi/3 (Al-Dasht, 2012)*

- **Profile (R5):**

Profile R5 consists of five sections (R5-1 to R5-5) as shown in Figure 1 extended to about 1100 m and located about 600m to the north of profile R4, and parallel to it. The inversion results are shown in Figure 12. The geoelectrical image shows a variation in resistivity distribution horizontally and vertically with resistivity values less than 1.4 Ωm to more than 250 Ωm. Resistivity values gradually change horizontally in section R5-1 to section R5-5 from the west to the east, where the range > 134 Ωm to the west that reduced to 50 Ωm at the east, due to the soil moister differences, and properties discrepancy that reflects the topsoil layer (sand and sandy clay). Below the top layer the apparent resistivity values are lower, which are determined by saline water intrusion coming from the coast and extends along the section R5-1 in the western side of a distance from (0 to 80 m) at shallow depths and decreases in the section R5-2 up to distance of 180 m eastward to a depth of about 12 m, where a brackish water zone can be seen clearly at section R5-3 and R5-4 at the same depth but not observed at section R5-5 (at 480m from the coast).

- **Profile (R6):**

Profile R6 was carried out in NW–SE direction, consists of five sections (R6-1 to R6- 5), extended to about 830 m and located about 600 m to the north of profile R5, and parallel to it.

The geoelectrical image Figure 13 shows horizontal layers and a variation in resistivity distribution, with resistivity values from less than 2 Ωm to more than 1951 Ωm. The top layer exhibits high resistivity (>500 Ωm) from the surface extended along profile due to the presence of coarse grained sediment sand on the surface.

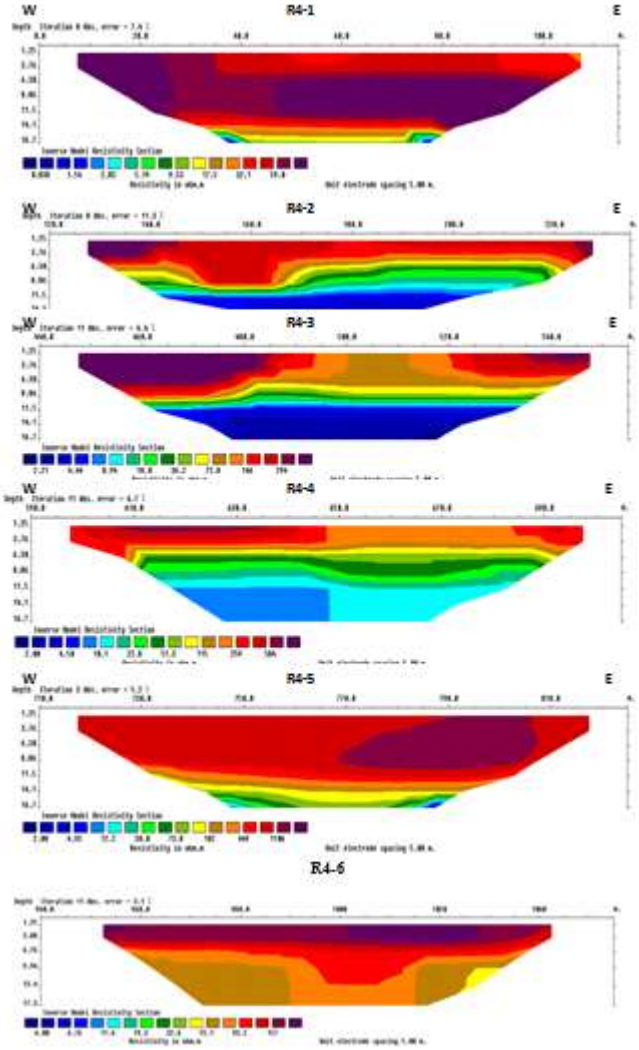

Figure 11 *2D Electrical resistivity images along profile R4*

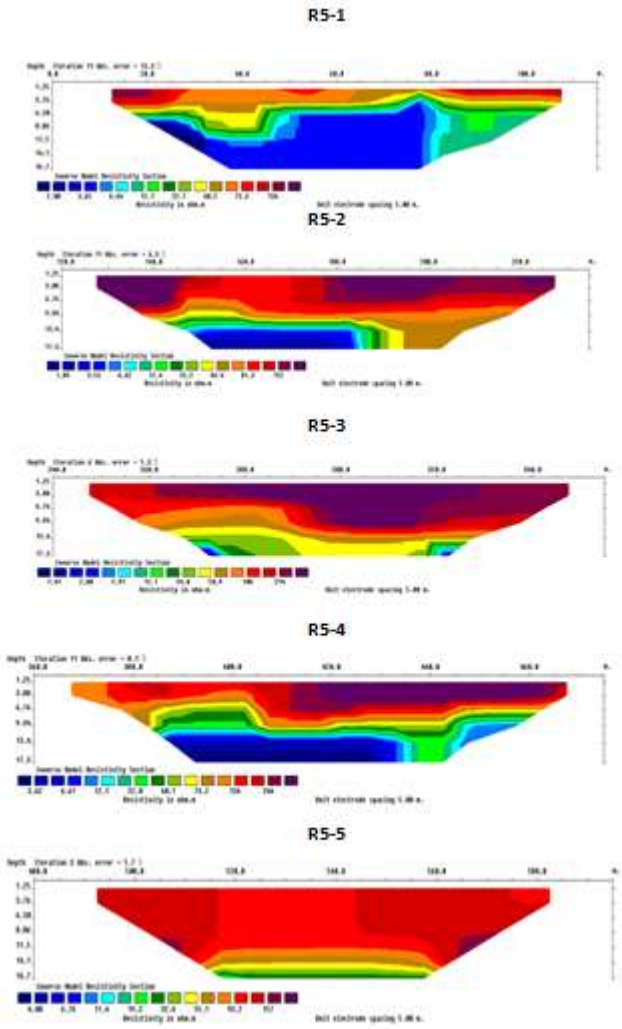

Figure 12 *2D Electrical resistivity images along profile R5*

The inverted models indicated a high conductive layer with low resistivity value (4 to 15Ωm) up to depth 13m from the surface that reflects a clay layer saturated with brackish water and extend along the section R6-1, and at depth more than 16m in section R6-2 at about 180m east of the coast but not observed after this distance.

The freshwater aquifer underlying the dry sand has a resistivity ranging between (15-75Ωm) detected at section R6-3, R6-4 and R6-5 at depths approximately under 11m.

The interpretation of VES S3 and S4 (Figures 14 and 15) indicate that freshwater appear at depth more than 20 m along R6-3, R6-4 and R6-5 sections that agreement with 2D inverse model of (R6).

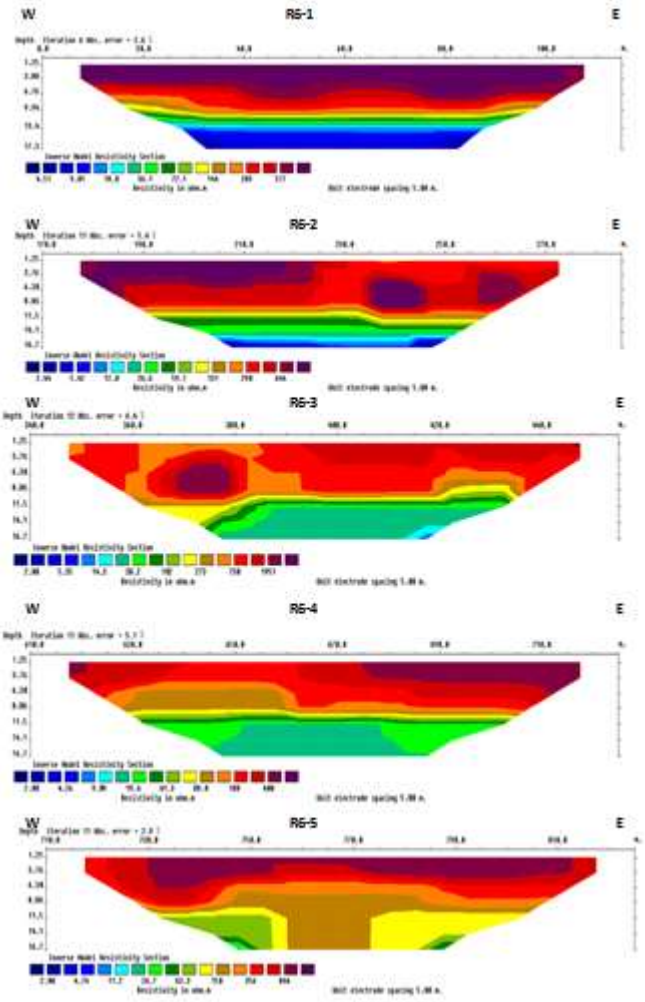

Figure 13 *2D Electrical resistivity images along profile R6*

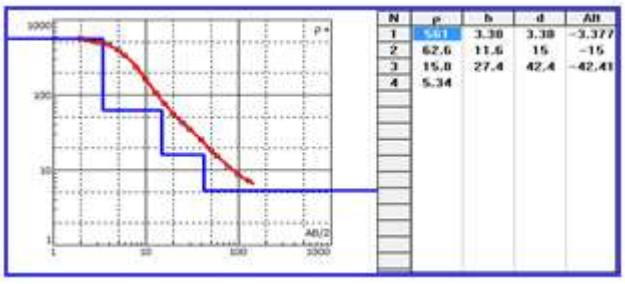

Figure 14 *1D geoelectrical model of VES S3*

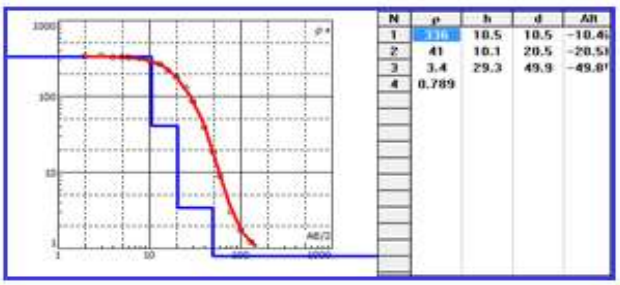

Figure 15 *1-D geoelectrical model of VES S4*

5. Conclusions:

Geophysical methods mainly electrical resistivity 2D is good tool to delineate seawater intrusion and for studying conductive bodies of hydrogeological interest and subsurface geological structural.

The geoelectrical image shows that Seawater intrusion (< 2 Ωm) in the aquifer mapped at shallow depths (3-6m) in the western sections near coastal line to depth of about 17m at about 1000m east of the coast line. Seawater intrusion cannot be observed in sections eastwards coastal line for more than this distance by the present 2D configuration due to the limited cable extension. From the interpreted geoelectrical section 1D and 2D images, we can conclude that seawater intrusion zone appears at the western part of the study area and extends along Rafah coastal with a difference distance and depths. The depths are ranging between (few meters to 20 m) in the western sections, while they are between (40 to more than 65 m) in the eastern section. Qualitative interpretation (1D) reveals that fresh water zone lies at the eastern part of the study area, where the fresh/ brackish aquifer thickness in the south (S1) is about 23m, increased to about 40 m northwards to (S3).

Acknowledgments:

The authors would like to thank the Middle East Desalination Research Centre (MEDRC), the Scientific Research at the Islamic University of Gaza and Palestinian Ministry of Education & Higher Education for the grants offered to achieve this research work.

References:

Abu El-Naeem, M. F. A., Abu Heen, Z. H., & Tubail, K. (2009). *Factors behind Groundwater Pollution by Nitrate in North Governorates of Gaza Strip (1994-2004)*. In Thirteenth International Water Technology Conference, IWTC13, Hurghada, Egypt.

Abu Heen, Z. H., & Muhsen, S. A. (2016). Application of Vertical Electrical Sounding for Delineation of Sea Water Intrusion into the Freshwater Aquifer of Southern Governorates of Gaza Strip, Palestine. *IUG Journal of Natural Studies*, *24*(2).

Abu Heen, Z. H., Abu El-Naeem, M., & Tubail, KH. (2008). Groundwater problems resulting from heavy pumping in north governorates of Gaza Strip (1999-2004). In *Twelfth International Water Technology Conference, IWTC12, Alexandria, Egypt,* p. 877-891.

Al-Absi, A. (2008). Nitrate contamination of ground water and methemoglobinemia in gaza strip. *J Al-Aqsa Unv*, *12*, 1-14.

Al-Agha, M. R., & Mortaja, R. S. (2005). Desalination in the Gaza Strip: drinking water supply and environmental impact. *Desalination*, *173*(2), 157-171.

Al-Bassam, A. M., & Hussein, M. T. (2008). Combined geo-electrical and hydro-chemical methods to detect salt-water intrusion. *Management of Environmental Quality*, *19*(2), 179-193.

Al-Dasht, J. (2012). *Hydrogeological Evaluation of the Aquifer in the Southern Part of the Gaza Strip, Palestine* (Unpublished Master Thesis). AL-Azhar University – Gaza, Palestine.

Basheer, A. A., Taha, A. I., Mansour, K. Q., Khalil, A., & Rabeh, T. (2014). Assessment of the Saline-Water Intrusion through the Fresh Groundwater Aquifer by Using ER and TEM Methods at the Qantara Shark Area, Sinai Peninsula, Egypt. *International Journal of Innovative Research and Development*, *3*(4), 398-406.

Batayneh, A., Elawadi, E., & Al-Arifi, E. (2010). Use of Geoelectrical Technique for Detecting Subsurface Fresh and Saline Water: A Case Study of the Eastern Gulf of Aqaba Coastal Aquifer, Jordan . *Journal of Coastal Research, 26(6), 1079–1084.*

Bobachev. (2010). *IPI2Win v.2.1, IPI_Res, IPI_Res3 Users Guide*. Moscow state university, Moscow.

Capizzi, P., Cellura, D., Cosentino, P., Fiandaca, G., Martorana, R., Messina, P., ... & VALENZA, M. (2010). Integrated hydrogeochemical and geophysical surveys for a study of sea-water intrusion. *Bollettino di Geofisica Teorica ed Applicata*, *51*(4), 285-300.

Chachadi, G., & Ferreiraj, I. (2005). *Assessing aquifer vulnerability to seawater intrusion using GALDIT method: Part 2- GALDIT indicators description*. The 4th Inter-Celtic Colloquium on Hydrology and Management of Water resources, Portugal.

Chitea, F., Georgescu, P., & Ioane, D. (2011). Geophysical detection of marine intrusions in Black Sea coastal areas (Romania) using VES and ERT data. *Geo-Eco-Marina*, *17*, 95-102.

Choudhury, K., & Saha, D. K. (2004). Integrated geophysical and chemical study of saline water intrusion. *Ground Water, 42*(5), 671-677.

Dahlin, T., & Zhou, B. (2004). A numerical comparison of 2D resistivity imaging with 10 electrode arrays. *Geophysical prospecting*, *52*(5), 379-398.

De Franco, R., Biella, G., Tosi, L., Teatini, P., Lozej, A., Chiozzotto, B., ... & Bassan, V. (2009). Monitoring the saltwater intrusion by time lapse electrical resistivity tomography: The Chioggia test site (Venice Lagoon, Italy). *Journal of Applied Geophysics*, *69*(3), 117-130.

Gemail, K., Samir, A., Oelsner, C., Mousa, S. E., & Ibrahim, S. (2004). Study of saltwater intrusion using 1D, 2D and 3D resistivity surveys in the coastal depressions at the eastern part of Matruh area, Egypt. *Near Surface Geophysics*, *2*(2), 103-109.

Geotomo Software. (2010). *Geoelectrical Imaging 2D & 3D*. Malaysia. Retrieved October 16, 2016, from: http://www.geoelectrical.com/

Himi, M., Stitou, J., Rivero, L., Salhi, A., Tapias, J. C., & Casas, A. (2010, September). *Geophysical surveys for delineating salt water intrusion and fresh water resources in the Oued Laou coastal aquifer*. In Near Surface 2010-16th EAGE European Meeting of Environmental and Engineering Geophysics. Zurich, Switzerland.

Kalisperi, D., Soupios, P., Kouli, M., Barsukov, P., Kershaw, S., Collins, P., & Vallianatos, F. (2009, February*). Coastal aquifer assessment using geophysical methods (TEM, VES), case study: Northern Crete, Greece*. In 3rd IASME/WSEAS international conference on geology and seismology (GES '09), Cambridge, UK.

Keller, G. V., & Frischknecht, F. C. (1966). *Electrical methods in geophysical prospecting*. Oxford: Pergamon Press Inc.

Lagudu, S., Rao, V. G., Prasad, P. R., & Sarma, V. S. (2013). Use of geophysical and hydrochemical tools to investigate seawater intrusion in coastal alluvial aquifer, Andhra Pradesh, India. In *Groundwater in the Coastal Zones of Asia-Pacific* (pp. 49-65). Netherland: Springer Netherlands.

Loke, M. (2004). *Electrical imaging surveys for environmental and engineering studies, a practical guide to 2D and 3D surveys*. Retrieved October 16, 2016, from: http://www.geoelectrical.com/

Metcalf & Eddy, (2009). Geophysical surveys in the Gaza Govornorates, unpublished report. Gaza, Palestine, pp:63.

Mogren, S. (2015). Saltwater Intrusion in Jizan Coastal Zone, Southwest Saudi Arabia, Inferred from Geoelectric Resistivity Survey. *International Journal of Geosciences*, 6(3), 286-297.

Muhsen, Sh., A. (2016). Hydrogeophysical investigation for the delineation of seawater intrusion ito the coastal freshwater aquifer of southern governorates, south of Gaza Strip, Palestine. Msc thesis, Islamic University of Gaza.

Olympia, K., George, V., & Konstantinos, V. (2012). Application of geophysical methods to detection of saline aquifers at the area of aggelochori, thessaloniki, Greece. *International Conference Protection and Restoration of the Environment XI, 298-307.*

PCBS-Palestinian Central Bureau of Statistics. (2016). *Statistical Yearbook of Palestine 2016*. No. 16. Ramallah, Palestine.

PWA - Palestinian Water Authority. (2013b). *Evaluation of Groundwater- Part B- Water Quality in the Gaza Strip Municipal Wells*, Internal report. Palestine.

PWA-Palestinian Water Authority. (2013a). *Groundwater wells in the Gaza Strip*, Arabic report. Palestine.

PWA-Palestinian Water Authority. (2014). *National Strategy for Water and Waste Water in Palestine*, Arabic Report. Palestine.

PWA-Palestinian Water Authority. (2015a). *2014 Water Resources Status Summary Report /Gaza Strip Water Resources Directorate.* Palestine.

PWA-Palestinian Water Authority. (2015b). *Water Resources Evaluation in Rafah, Gaza Strip 2014*, Arabic Report. Palestine.

Sherif, M., El Mahmoudi, A., Garamoon, H., Kacimov, A., Akram, S., Ebraheem, A., & Shetty, A. (2006). Geoelectrical and hydrogeochemical studies for delineating seawater intrusion in the outlet of Wadi Ham, UAE. *Environmental geology*, *49*(4), 536-551.

Shomar, B. (2011). Retracted Article: Groundwater contaminations and health perspectives in developing world case study: Gaza Strip. *Environmental geochemistry and health*, *33*(2), 189-202.

Thabit, J. M., & AL-Hameedawie, M. M. (2014). Delineation of groundwater aquifers using VES and

2D imaging techniques in north Badra area, Eastern Iraq. *Iraqi J. of Science*, *55*(1), 174-183.

UNCT- United Nations Country Team. (2012). *Gaza in 2020 A liveable place*. Palestine.

Yassin, M. M., Amr, S. S. A., & Al-Najar, H. M. (2006). Assessment of microbiological water quality and its relation to human health in Gaza Governorate, Gaza Strip. *Public Health*, *120*(12), 1177-1187.

Zohdy, A., Eaton, G., and Mabey, D. (1974). Application of Surface Geophysics to Groundwater Investigations. In D. Peck (Ed), *Techniques of Water-Resources Investigations of the U.S. Geological Survey "Book 2"* (p. 116). USA: USGS–TWRI.

استخدام طريقة المقاومة الكهربائية ثنائية البعد لتحديد خصائص مياه البحر الشاطئية المتداخلة في الخزان الجوفي لمحافظة رفح, جنوب قطاع غزة, فلسطين

تعتبر طرق المقاومة الكهربائية وخاصة ثنائية البعد وأحادية البعد الطرق الرئيسية المستخدمة لتحديد ومتابعة تداخل مياه البحر المالحة في الخزان الجوفي العذب. استخدم في الدراسة الحالية ثلاثون قطاعا ثنائي البعد نفذت بترتيب وينر- شلمبرجير (باتجاه شمال غرب- جنوب شرق) موزعة على ستة بروفيلات متعامدة على شاطئ البحر للجزء الجنوبي من الخزان الساحلي لقطاع غزة (محافظة رفح), وقد نفذت أيضا أربعة نقاط قياس أحادية البعد بترتيب شلمبرجير وذلك بهدف تحديد مدى تداخل مياه البحر في الخزان الجوفي الساحلي الضحل للمنطقة ودراسة التكوينات الجيولوجية. أظهرت النتائج ان مياه البحر المالحة تسود في المنطقة الغربية للدراسة وعلى طول شاطئ رفح على مسافات وأعماق مختلفة تتراوح بين عدة أمتار إلى 20 مترا في الناحية الغربية بينما تزداد إلى اعماق بين 40 إلى أكثر من 65 مترا شرقا. أظهرت نتائج المسح الكهربائي تطابقا ممتازا مقارنة مع النتائج المأخوذة من ثلاثة أبار محفورة في المنطقة إضافة الى نتائج التحاليل الكيميائية لثلاث عينات من المياه تم تحليلها.

كلمات مفتاحية:
المقاومة الكهربائية ثنائية البعد،
المقاومة الكهربائية العمودية،
تداخل مياه البحر،
رفح،
قطاع غزة،
فلسطين.